

Matter in Toy Dynamical Geometries

Tomasz Konopka

ITP, Utrecht University, Utrecht 3584 CE, the Netherlands

E-mail: t.j.konopka@uu.nl

Abstract. One of the objectives of theories describing quantum dynamical geometry is to compute expectation values of geometrical observables. The results of such computations can be affected by whether or not matter is taken into account. It is thus important to understand to what extent and to what effect matter can affect dynamical geometries. Using a simple model, it is shown that matter can effectively mold a geometry into an isotropic configuration. Implications for “atomistic” models of quantum geometry are briefly discussed.

1. Introduction

In the context of quantum gravity (see e.g. [1] for an overview of different approaches), much attention is devoted to studies of pure-gravity systems in which all matter degrees of freedom and their interactions are switched off. Whereas the use of this assumption is understandable given that most proposals for quantum theory of gravity are difficult to study even without the inclusion of additional fields, it is known that the presence of matter can alter the behavior of a gravitational system [2]. The purpose of this paper is to illustrate the effect of matter on geometry in a simple setting. In particular, the purpose is to show that matter can induce isotropy in a model that does not assume it a-priori - an effect not easily seen from standard treatments of matter in dynamical geometries [2].

Physical theories are often formulated using the Feynman path integral and many candidates for a theory of quantum gravity [1] are also defined within this framework. These candidates propose to study path integrals (partition functions) formally written as

$$Z_\phi = \int \mathcal{D}[g] \int \mathcal{D}[\phi] e^{-E(g, \phi)} \quad (1)$$

where integrals denote summations over geometries g and matter degrees of freedom ϕ , and $E(g, \phi)$ is a weighting function that depends on both the geometry and the matter content (this function can be interpreted as the action or the energy of the system, according to the setting). The weighting function is often assumed to be of the form $E(g, \phi) = E_g(g) + E_\phi(g, \phi)$ so that the contribution from the matter fields in $E_\phi(g, \phi)$ is separated from the pure-geometry part $E_g(g)$. Furthermore, it is often assumed that if the matter contribution $E_\phi(g, \phi)$ is set to zero, the resultant, simpler, path integral

$$Z_{\phi=0} = \int \mathcal{D}[g] e^{-E_g(g)} \quad (2)$$

has many of the same properties as the original one (1). That is, it is assumed that expectation values $\langle \mathcal{O} \rangle_\phi$ and $\langle \mathcal{O} \rangle_{\phi=0}$ of a geometric observable \mathcal{O} computed in the two models have similar

properties. It is this assumption that motivates the study of “pure-geometry” systems even when the real universe is known to contain matter fields of various types.

The purpose of this paper is to demonstrate that geometric observables can in fact be different depending on whether or not matter is included in the calculation. The strategy to demonstrate this will be to compute expectation values explicitly in the setting of a two dimensional rectangular box in which the sides lengths L_x and L_y are variable but the total area $L_x L_y = A$ is fixed. This system was already introduced in [3] but it is explored here more fully. An important property of this system is that it contains a single configuration where $L_x = L_y$ and the box is a square but it contains a multitude of other configurations in which $L_x \neq L_y$; the geometric observable $R = L_x/L_y$ differentiates the square configuration from the non-square ones. The main result will be that the expectation value for this ratio in a system without matter must be different from one, but that it can be one when matter is present.

The rest of the paper is organized as follows. Sec. 2 describes the flexible box system and defines its sum over geometries. The expectation value of the observable in the absence of matter is also computed. Sec. 3 discusses the effect of adding particles. It is shown through numerical studies that the expectation value of the observable $R = L_x/L_y$ in the presence of particles can be close to unity. This indicates that matter can select a homogenous and isotropic geometry from the ensemble. In Sec. 4 this discussion is extended to the case of fields and it shown in what circumstances the Casimir energy of fields has a similar effect. A discussion of applications to current research programs on “atomistic” models¹ of spacetime are presented in Sec. 5.

2. Toy Dynamical Geometries

2.1. Regularized Sum Over Geometries

Formal expressions like (1) and (2) do not specify the space of geometries to be integrated over or how exactly to carry out the integrals. To overcome this, several approaches (e.g. [3–5]) propose to study systems like (1) in a discretized setting. In those approaches, one replaces the integral over geometries by a finite sum over a set \mathcal{C} of geometry configurations. The same strategy is adopted here. Since the purpose of this paper is to study effects of matter on dynamical geometries and not to propose a sensible way or regularizing the path integral for quantum gravity, the set \mathcal{C} is chosen to make this specific application possible.

Consider configurations spaces \mathcal{C}_A corresponding to sets describing rectangular boxes having sides of length L_x and L_y and area A . To make each of these sets \mathcal{C}_A finite, the possible lengths L_x and L_y must be restricted to a discrete or semi-discrete spectrum characterized by at least one length scale, ℓ , designating a smallest allowed length. If the allowed lengths are assumed to be equally spaced when they are small, a concrete length spectrum that can be used is

$$L \in \begin{cases} \mathbb{N}\ell & \text{if } L \leq \lambda \\ \mathbb{R} & \text{if } L > \lambda. \end{cases} \quad (3)$$

The minimal value and next larger values for L are ℓ and integer multiples of ℓ , respectively, up to a scale λ . Above this scale, L can take any real number value. It will be convenient to choose $\lambda = \sqrt{A}$. With this convention, the sets \mathcal{C}_A can be written out explicitly as

$$\mathcal{C}_A = \left\{ \left(\ell, \frac{A}{\ell} \right), \left(2\ell, \frac{A}{2\ell} \right), \dots, \left(\sqrt{A}, \sqrt{A} \right), \dots, \left(\frac{A}{\ell}, \ell \right) \right\}. \quad (4)$$

Note that these sets are countable and well defined for all real $A > \ell^2$.

¹ The term “atomistic” model is due to H-T. Elze.

2.2. Partition Function and Geometric Observables

After defining the configuration space of a dynamical box with area A , one must specify how the configurations should be weighted in the ensemble defining the partition function (1). In the case where they are all equally weighted, the partition function of the system is

$$Z = \sum_{p=1}^{\lambda/\ell} (1 + 1) = \frac{2\lambda}{\ell} = \frac{2\sqrt{A}}{\ell}. \quad (5)$$

The first term shown in the sum represents values of L_x in the discrete part of the length spectrum, i.e. the first half of the configurations listed in (4). The second term is the analogous sum over discrete values of L_y^2 . In the end, Z turns out to be equal to the size of the set \mathcal{C}_A ; the thermodynamic properties of the empty box system are determined entirely by entropy.

Expectation values of observables describing the box geometry can now be computed. For concreteness, consider the ratio $R = L_x/L_y$. The expectation value for R should be close to unity if the box is likely to be square, and very different from unity if the box is likely to be long and narrow. One finds

$$\langle R \rangle = \frac{1}{AZ} \left[\sum_{p=1}^{\lambda/\ell} \left((p\ell)^2 + \left(\frac{A}{p\ell} \right)^2 \right) \right] \rightarrow \frac{\pi^2 \sqrt{A}}{12\ell}. \quad (6)$$

The last expression denotes the evaluation of $\langle R \rangle$ in the limit $A \rightarrow \infty$. Since the result is divergent in this limit, (also when $\ell \rightarrow 0$), the calculation suggests that the box should be expected to be long and narrow in that limit. Curiously, note that the expectation value for the inverse ratio, $\langle L_y/L_x \rangle$, is given by exactly the same diverging expression; this is a consequence of the $L_x \leftrightarrow L_y$ symmetry of the system and implies that these ratios provide measures for the degree to which the two sides of the box are different and cannot be used to infer which length, L_x or L_y , is larger.

Another useful expectation value is

$$\langle R^2 \rangle = \frac{1}{A^2 Z} \left[\sum_{p=1}^{\lambda/\ell} \left((p\ell)^4 + \left(\frac{A}{p\ell} \right)^4 \right) \right] \rightarrow \frac{\pi^4 A^{3/2}}{180 \ell^3}; \quad (7)$$

the last expression again stands for the $A \rightarrow \infty$ limit. This quantity can be used to compute the fluctuations $(\Delta R)^2 = \langle R^2 \rangle - \langle R \rangle^2$ of the ratio R . In the limit $A \rightarrow \infty$, the contribution to $(\Delta R)^2$ from the first term, $\langle R^2 \rangle$, is much larger than that from the second, $\langle R \rangle^2$, and thus the fluctuations diverge as $A^{3/2}$.

3. Particles in Dynamical Geometries

3.1. Particles as Standing Waves

Suppose that the flexible box is populated with quantum mechanical particles of mass m . The dynamics of each particle is described by the Schrodinger equation in two dimensions with a potential that is zero inside the box and infinity everywhere else. After setting $\hbar = c = 1$, the energy spectrum for each particle is

$$E = \frac{1}{2m} (k_x^2 + k_y^2), \quad (8)$$

² The given prescription for evaluating Z carries a risk of over-counting whenever the two configurations corresponding to $p = \lambda/\ell$ are in fact equivalent. This problem can be averted by considering A such that λ/ℓ is not an integer. In any case, the error involved becomes negligible when the area is large.

where k_x and k_y are the momenta in the x and y directions, respectively. The allowed values for these momenta ($i = x, y$) are

$$k_i = \frac{(2 - \sigma)\pi n_i}{L_i} \quad (9)$$

where σ depends on the type of boundary conditions,

$$\sigma = \begin{cases} 1 & \text{Dirichlet} \\ 0 & \text{Periodic,} \end{cases} \quad (10)$$

and $n_i = \sigma, 1, 2, \dots$ are quantum numbers whose range also depends on the boundary conditions.

For a given box configuration (L_x, L_y) , the partition function for a single particle is

$$z(L_x, L_y) = \sum_{n_x=\sigma}^{\infty} \exp\left(-\frac{\beta(2-\sigma)^2\pi^2 n_x^2}{2mL_x^2}\right) \sum_{n_y=\sigma}^{\infty} \exp\left(-\frac{\beta(2-\sigma)^2\pi^2 n_y^2}{2mL_y^2}\right) \quad (11)$$

where $\beta = 1/kT$ is the inverse temperature. For a system of N identical Maxwell-Boltzmann particles, their combined contribution is

$$z_N(L_x, L_y) = (z(L_x, L_y))^N / N! \quad (12)$$

The total partition for the particles as well as the box can then be written as

$$Z = 2 \sum_{p=1}^{\lambda/\ell} z_N\left(p\ell, \frac{A}{p\ell}\right) \quad (13)$$

where the factor of two in front has the same origin as in (5).

It is important to emphasize here that z and z_N depend explicitly on the lengths of the sides of the box and the parameter σ . In particular, it can be shown that the largest term in Z is due to configurations with $L_x = L_y$ when $\sigma = 1$, or to configurations with $L_x \gg L_y$ and $L_y \gg L_x$ when $\sigma = 0$. These features form the basis for understanding the results described next.

3.2. Evaluation of Observables

The expectation value for R can now be computed, analogously to (6), using

$$\langle R \rangle = \frac{1}{ZA} \sum_{p=1}^{\lambda/\ell} \left((p\ell)^2 + \left(\frac{A}{p\ell} \right)^2 \right) z_N\left(p\ell, \frac{A}{p\ell}\right). \quad (14)$$

This can be evaluated numerically given certain values for the parameters. To make for a realistic situation, the mass of the particles and the temperature of the system should be much smaller than the inverse minimal length, $m, kT \ll 1/\ell$. Thus $\beta(2 - \sigma)^2\pi^2/8m \gg 1/\ell^2$. After fixing this ratio in terms of ℓ , which can then be set to unity without loss of generality, the remaining free variables are A and N . In the following, the number of particles N is expressed in the form $N = N_0 + cA^\alpha$ with N_0 and α positive dimensionless constants, and c a positive constant with dimension depending on the value of α .

Numerical results for $\langle R \rangle$ and $(\Delta R)^2$ with $\ell = 1$, $\beta(2 - \sigma)^2\pi^2/8m = 10$ are shown in Fig. 1. Curves corresponding to a fixed number of particles ($N = 1, \sigma = 0, 1$) show that the expectation value $\langle R \rangle$ and its fluctuations rise as the area of the boxes is increased. The asymptotic slopes match the behavior expected from the empty box calculations in (6) and (7). Curves corresponding to systems wherein the number of particles scales with area ($N = 0.01A, \sigma = 0, 1$)

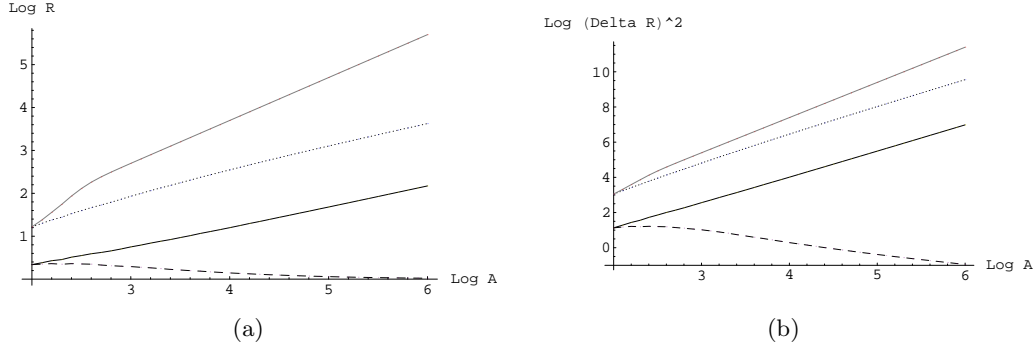


Figure 1. Geometric observables in toy geometries. In both plots, the lines represent (top to bottom) systems with $(N, \sigma) = (0.01A, 0), (1, 0), (1, 1), (0.01A, 1)$.

exhibit more interesting behavior. When Dirichlet boundary conditions are imposed ($\sigma = 1$), the asymptotic behavior for large A is $\langle R \rangle \rightarrow 1$ and $\langle (\Delta R)^2 \rangle \rightarrow 0$. Thus, in this case, the ensemble of particles mold the dynamical geometry into a stable isotropic configuration. The situation is different for periodic boundary conditions ($\sigma = 0$); there both the expectation value for R and its fluctuations diverge faster than in the empty box situations.

The most interesting result of these plots is the emergence of isotropy, $\langle R \rangle \rightarrow 1$, in the case of Dirichlet boundary conditions. It can be understood qualitatively as follows. The isotropic configuration contributes the most out of all the terms composing the partition function $z(L_x, L_y)$ of a single particle. This advantage is then raised to a power cA^α . Since the number of non-isotropic configurations grows at most polynomially with A (it grows as \sqrt{A}), all of those configurations contribute negligibly to the overall partition function in the large area limit. The difference in growth rates between the polynomial and the exponential components also explains why the approach to perfect isotropy occurs rather quickly.

4. Casimir Energy in Dynamical Geometries

4.1. Regularization of Casimir Energy

Another way of implementing matter is using fields instead of particles. The expectation value of the Hamiltonian operator of a field is in general given by a sum of two terms: one term proportional to the number of particles in some state (zero for the vacuum), and one other term that is divergent even in the absence of physical particles. This latter term is called the Casimir energy and it is usually attributed to quantum vacuum fluctuations [7]. It is (setting $\hbar = c = 1$)

$$E_C = \frac{\eta}{2} \sum_i \omega_i. \quad (15)$$

The factor η is positive for bosonic fields and negative for fermionic fields. It is different from one if a field (such as a vector field) can have multiple polarizations. The summation is over all field mode energies.

In a flat 2 + 1 dimensional background, relativistic field modes have energies ω given by $\omega^2 = m^2 + k_x^2 + k_y^2$ in terms of momenta $k_{x,y}$ and mass m . The momenta are again constrained by boundary conditions given in (9) and (10). Thus the Casimir energy is

$$E_0 = \frac{1}{2} \eta \pi (2 - \sigma) \sum_{n_x=\sigma}^{\infty} \sum_{n_y=\sigma}^{\infty} \left(\tilde{m}_\sigma^2 + \frac{n_x^2}{L_x^2} + \frac{n_y^2}{L_y^2} \right)^{1/2}, \quad (16)$$

where $\tilde{m}_\sigma = m/(2 - \sigma)\pi$. This quantity is ultra-violet divergent; much work on the Casimir energy revolves around extracting its physically relevant components [7]. One technique to do this is to define a modified version of the summation (16) which includes a cutoff function D_ℓ multiplying each summand as follows:

$$E_{0,\ell} = \frac{1}{2} \eta \sum_{n_x=\sigma}^{\infty} \sum_{n_y=\sigma}^{\infty} \omega_{n_x, n_y} D_\ell \left(\frac{n_x}{L_x}, \frac{n_y}{L_y} \right). \quad (17)$$

The cutoff function D_ℓ must be chosen to satisfy certain criteria [8]. First, it must reduce to unity when $\ell \rightarrow 0$ so that $E_{0,\ell} \rightarrow E_0$ in this limit. Second, for $\ell \neq 0$, the function should fall off quickly when its arguments become large as to make $E_{0,\ell}$ finite. Third, it should not have any singularities or branch cuts in the complex plane. Lastly, it is also convenient to choose D_ℓ so that it is symmetric in its arguments, $n_x/L_x \leftrightarrow n_y/L_y$.

To evaluate (17), one applies the Abel-Plana formula

$$\sum_{n=0}^{\infty} F(n) = \int_0^{\infty} F(t) dt + \frac{1}{2} F(0) + i \int_0^{\infty} \frac{dt}{e^{2\pi t} - 1} (F(it) - F(-it)) \quad (18)$$

twice in order to exchange the two summations over n_x and n_y into integrals. The resultant $E_{0,\ell}$ can be written (see [7–9] for more details) in the form

$$E_{0,\ell} = \frac{1}{2} \eta \pi (2 - \sigma) (E_{\ell,A} + E_{\ell,B} + E_{AR}). \quad (19)$$

The first two terms in the parenthesis are

$$\begin{aligned} E_{\ell,A} &= (L_x L_y) \int_0^{\infty} du_x \int_0^{\infty} du_y \sqrt{\tilde{m}_\sigma^2 + u_x^2 + u_y^2} D_\ell(u_x, u_y) \propto \frac{L_x L_y}{\ell^3} \\ E_{\ell,B} &= \frac{1}{2} (1 - 2\sigma) (L_x + L_y) \int_0^{\infty} du \sqrt{\tilde{m}_\sigma^2 + u^2} D_\ell(u, 0) \propto (1 - 2\sigma) \frac{L_x + L_y}{\ell^2}. \end{aligned} \quad (20)$$

These terms are divergent when $\ell \rightarrow 0$ and thus parametrize the ultra-violet behavior of E_0 . When $\ell \neq 0$ and $m \ll 1$, their leading behavior is as shown. The precise coefficients are dependent on the details of the cutoff function. Interestingly, the terms are proportional to the area and perimeter of the two-dimensional box, and the latter has different sign for the two considered boundary conditions.

The last term in (19), E_{AR} , consists of the remaining contributions obtained from the expansions using the Abel-Plana formula. For the present discussion, the important features of E_{AR} are that it is finite in the $\ell \rightarrow 0$ limit and that its magnitude decreases with area [6, 7, 9].

The Casimir energy is an active subject of research [6, 7] because it is a purely quantum effect that leads to a macroscopic effect in the form of the Casimir effect/force. In the standard description of the Casimir effect, it is the finite term E_{AR} that is physically interesting. A clear explanation of why the divergent terms can be discarded when describing situations relevant for experiments testing the Casimir force is given in works on cavities with a piston [8]. In short, the reason is that the divergent contributions from inside and outside a cavity cancel from formulae describing measurable quantities (the force on the piston).

In the context considered in this paper, the field is defined only within the boundaries of the box, and thus a cancellation of divergent terms from inside and outside cannot occur. The analysis of the effect of Casimir energy on the statistical properties of the dynamical box must therefore either include the regularized divergent terms, or discard them in an ad-hoc manner.

4.2. Casimir Energy and Expected Geometry

The partition function of the flexible box with field is

$$Z = 2 \sum_{p=1}^{\sqrt{A}/\ell} z_{\phi}(\beta, p) \quad (21)$$

where $z_{\phi}(\beta, p)$ stands for the partition function of a field theory at inverse temperature β in a box configuration labelled by p . $z_{\phi}(\beta, p)$ should have contributions from the Casimir energy and also from the real particle present in a thermal state. However, in the low temperature regime where the average thermal energy is smaller than the mass of the particles, it is reasonable to approximate z_{ϕ} by the contribution from the Casimir energy alone. Thus $z_{\phi}(\beta, p) \sim e^{-\beta E_0(p)}$ with E_0 given by (19) for each box configuration labelled by p .

Consider first the option of including the divergent but regularized terms of E_0 in the calculations. Since the area of the boxes is kept fixed, the term $E_{\ell,A}$ contributing to E_0 is the same for all the box configurations and so can be factored out and essentially ignored. The other terms depend on the geometry of the box and thus must all be taken into consideration. Being divergent in the $\ell \rightarrow 0$ limit, the term $E_{\ell,B}$ proportional to the perimeter of the box is dominant over the term E_{AR} . The latter term can therefore be ignored. The partition function thus becomes

$$Z = 2 \sum_{p=1}^{\lambda/\ell} \exp \left(-\beta \eta \pi (2 - \sigma) (1 - 2\sigma) \frac{1}{\ell^2} \left(p\ell + \frac{A}{p\ell} \right) \right). \quad (22)$$

Expectation values can be computed numerically similarly as done in the previous section. The results are that the square configuration become dominant if the parameters σ and η are chosen as either $\sigma = 1$ and $\eta < 0$, or as $\sigma = 0$ and $\eta > 0$. That is, the square configuration is preferred if either the field is fermionic with Dirichlet boundary conditions or if the field is bosonic with periodic boundary conditions.

Next, consider the option of discarding the regularized divergent terms of E_0 and using only the finite contribution E_{AR} . Since E_{AR} is decreasing with A , it's effect would be insignificant in the partition function for the dynamical box. The statistical properties of the dynamical box should thus be expected to match those described in Sec. 2. In other words, the finite component of the Casimir energy is not sufficient for shaping the dynamical geometry into a particular preferred configuration.

5. Discussion

Any successful theory of quantum dynamical geometry must eventually include coupling to the matter content observed in the universe. A-priori, average properties of dynamical geometries should be expected to be different when computed in theories with and without matter. Consequently, it is important to understand in detail the way in which matter may affect geometric observables. This issue was addressed in this paper using a toy model in which dynamical geometry was described by a two-dimensional “flexible” rectangular box of fixed area A . The expectation value of the observable $R = L_x/L_y$ was shown to be very different depending on whether matter was present or not, and depending on the boundary conditions imposed on the matter. In particular, in the presence of a finite density of particles and Dirichlet boundary conditions, it was shown that $\langle R \rangle$ can approach unity and the fluctuations $(\Delta R)^2$ can vanish in the large area limit. This scenario can thus be argued to give rise to a classical, stable, and isotropic geometry. A similar effect can arise also in the case of quantum fields if the divergent but regularized Casimir energy is included in the analysis.

The purpose of the calculations presented in this paper is to exemplify *that* and illustrate *how* matter can affect a dynamical geometry. One technical assumption that was used regarded

the form of the spectrum for the lengths L_x and L_y . Although the spectrum was chosen only for convenience and not according to a deep physical principle, it should be possible to formulate precisely the conditions that must be satisfied by the physical length spectrum for the results presented to continue to hold. This kind of analysis, however, goes beyond the scope of this paper. Nonetheless, it is worth pointing out that the spectrum used is a natural one from the point of view of “atomistic” models of spacetime models in which large-scale geometry is thought of being composed of a large number of elementary building blocks.

A natural application of the presented ideas is in the context of “atomistic” models of spacetime. In this context, conventional approaches to studying matter on dynamical geometries (see e.g. [2]) have limited use because the notion of geometry is only emergent, but the general mechanism described in this paper can be applied. Consider for example the class of models called graphity [3, 4]: the basic version of these models does not generate extended manifold-like graphs, but modified versions that include a homogeneity requirement do [3]. It has been suggested that matter degrees of freedom might provide such a homogeneity requirement via a mechanism similar to the one described here. Similarly, it is possible that matter might play an important role in other models of emergent spacetime such as causal sets [10, 11] or group field theory [12].

Another application of the ideas presented here is in cosmology: instead of putting homogeneity and isotropy as inputs in an ansatz for a cosmological spacetime solution, it may be interesting to see them arising from the statistical mechanics of matter fields.

Acknowledgments

I would like to thank the organizers of DICE 2008 for a diverse and extremely stimulating workshop. I have also benefitted from discussions with J. Ambjorn and B. Z. Foster.

- [1] Oriti D, ed. 2008 *Approaches to Quantum Gravity*, Cambridge University Press.
- [2] Birrell ND and Davies PC 1982 *Quantum fields in curved space*, Cambridge University Press.
- [3] Konopka T, Phys. Rev. D **78**, 044032 (2008) [arXiv:0805.2283 [hep-th]].
- [4] Konopka T, Markopoulou F and Severini S, Phys. Rev. D **77**, 104029 (2008) [arXiv:0801.0861 [hep-th]].
- [5] Ambjorn J, Jurkiewicz J and Loll R, Phys. Rev. Lett. **85**, 924 (2000). [arXiv:hep-th/0002050].
- [6] Milton KA, J. Phys. A **37**, R209 (2004). [arXiv:hep-th/0406024].
- [7] Bordag M, Mohideen U and Mostepanenko VM, Phys. Rept. **353**, 1 (2001) [arXiv:quant-ph/0106045].
- [8] Cavalcanti RM, Phys. Rev. D **69**, 065015 (2004) [arXiv:quant-ph/0310184].
- [9] Ambjorn J and Wolfram S, Annals Phys. **147**, 1 (1983).
- [10] Rideout D and Wallden P, arXiv:0810.1768 [gr-qc].
- [11] Johnston S, Class. Quant. Grav. **25**, 202001 (2008) [arXiv:0806.3083 [hep-th]].
- [12] Oriti D, arXiv:0710.3276 [gr-qc].